OXFORD

ORIGINAL ARTICLE

Slow Progressive Accumulation of Oligodendroglial Alpha-Synuclein (α-Syn) Pathology in Synthetic α-Syn Fibril-Induced Mouse Models of Synucleinopathy

Norihito Uemura ⬤, MD, PhD, Maiko T. Uemura, MD, PhD, Angela Lo, Fares Bassil, PhD, Bin Zhang, MD, PhD, Kelvin C. Luk, PhD, Virginia M.-Y. Lee, PhD, Ryosuke Takahashi, MD, PhD, and John Q. Trojanowski, MD, PhD

Abstract

Synucleinopathies are composed of Parkinson disease (PD), dementia with Lewy bodies (DLB), and multiple system atrophy (MSA). Alpha-synuclein (α-Syn) forms aggregates mainly in neurons in PD and DLB, while oligodendroglial α-Syn aggregates are characteristic of MSA. Recent studies have demonstrated that injections of synthetic α-Syn preformed fibrils (PFFs) into the brains of wild-type (WT) animals induce intraneuronal α-Syn aggregates and the subsequent interneuronal transmission of α-Syn aggregates. However, injections of α-Syn PFFs or even brain lysates of patients with MSA have not been reported to induce oligodendroglial α-Syn aggregates, raising questions about the pathogenesis of oligodendroglial α-Syn aggregates in MSA. Here, we report that WT mice injected with mouse α-Syn (m-α-Syn) PFFs develop neuronal α-Syn pathology after short postinjection (PI) intervals on the scale of weeks, while oligodendroglial α-Syn pathology emerges after longer PI intervals of several months. Abundant oligodendroglial α-Syn pathology in white matter at later time points is reminiscent of MSA. Furthermore, comparison between young and aged mice injected with m-α-Syn PFFs revealed that PI intervals rather than aging correlate with oligodendroglial α-Syn aggregation. These results provide novel insights into the pathological mechanisms of oligodendroglial α-Syn aggregation in MSA.

Key Words: Glial cytoplasmic inclusion, Multiple system atrophy, Oligodendrocyte, Parkinson disease, Preformed fibrils, Propagation.

INTRODUCTION

Alpha-synuclein (α-Syn) forms misfolded aggregates in a group of neurodegenerative diseases collectively known as synucleinopathies, including Parkinson disease (PD), dementia with Lewy bodies (DLB), and multiple system atrophy (MSA) [1, 2]. PD and DLB are thought to be a spectrum of disorders characterized by intraneuronal α-Syn aggregates called Lewy bodies [3]. PD is a movement disorder caused by dopaminergic neuron loss in the substantia nigra pars compacta. Patients who develop dementia before or within 1 year after the onset of motor symptoms of PD are clinically diagnosed as DLB [4]. However, MSA is clinically and pathologically distinct from PD and DLB. Patients with MSA mainly show parkinsonism, cerebellar ataxia, and autonomic failure; their clinical condition declines faster and overall survival is shorter than PD and DLB [5]. The pathological hallmark of MSA is abundant oligodendroglial α-Syn aggregates, referred to as glial cytoplasmic inclusions (GCIs), with rare neuronal inclusions [5].

α-Syn, a natively unfolded protein expressed mainly by neurons and rarely by glia, tends to form β-sheet-rich amyloid fibrils when it accumulates in the context of genetic overexpression or impaired degradation [6, 7]. In this context, several lines of α-Syn transgenic mice driven by oligodendrocyte-specific promoters were generated to model MSA in mice [8–10]. These mice exhibited some phenotypes characteristic of MSA such as motor disturbance and GCI-like oligodendroglial α-Syn aggregates in their brains. However, it is unclear to what extent these models replicate the pathological mechanisms of MSA because there is no evidence of elevation in α-Syn expression in the brain regions harboring GCIs or in oligodendrocytes in patients with MSA [11–13]. Indeed, the vast majority of cases with MSA are sporadic, and only a few gene mutations and single nucleotide polymorphisms have been reported to increase the risk of MSA [13–16]. Thus, the pathological mechanisms of MSA remain largely unknown.

Recent accumulating evidence suggests that neurodegenerative diseases caused by pathological proteins such as α-Syn, tau, and Aβ share common pathological mechanisms (17, 18). First, these misfolded protein aggregates serve as templates to recruit endogenous normal proteins and propagate intercellularly in a prion-like fashion. Second, heterogeneity of diseases caused by a single pathological protein can be, at least partly, explained by distinct conformations of the protein referred to as "strains." Injections of synthetic α-Syn preformed fibrils (PFFs) or brain lysates of patients with PD or DLB into the brains of rodents and nonhuman primates induces intraneuronal α-Syn aggregates similar to LBs and subsequent interneuronal spreading in the animal brains (19–23). Previous studies, including our recent study, demonstrated that pathological α-Syn aggregates of GCIs have distinct conformations and biological activities both in vitro and in vivo from those of LBs (24, 25). However, injections of brain lysates of patients with MSA into the brains of wild-type (WT) mice failed to replicate the oligodendroglial α-Syn pathology, raising questions about the pathogenesis of MSA (24–26).

In this study, we found slow progressive oligodendroglial α-Syn pathology in the brains of WT mice injected with mouse α-Syn (m-α-Syn) PFFs. To the best of our knowledge, this is the first report on development of oligodendroglial α-Syn aggregates in WT mice which resemble ones seen in human synucleinopathies. Moreover, our chronological analyses of the α-Syn PFF-injected mice provide novel insights into the pathological mechanisms of oligodendroglial α-Syn aggregation in MSA.

MATERIALS AND METHODS

Animals and Ethics Statement

Mouse olfactory bulb injections and following analyses were conducted at Kyoto University. C57BL/6J male mice at 2 months of age (purchased from Japan SLC, Shizuoka, Japan) were used (n = 42). All experimental procedures used in this study followed Japanese national guidelines. The Animal Research Committee of Kyoto University granted ethical approval and permission (MedKyo 17184).

Mouse dorsal striatum injections and following analyses were conducted at University of Pennsylvania. C57BL/6 C3H (B6C3) female mice at 2–3 months of age (n = 9) were used, and C57BL/6 female mice at the age of 2–3 months (n = 8) and 12–16 months (n = 12) were used as young and aged mice, respectively. The rationale is that mouse maturation continues until ~3 months of age, but it is not until mice are >6 months old that they begin to exhibit age-related changes, and mice are considered to be "middle-aged" by ~10 months of age (27). B6C3 mice and young C57BL/6 mice were purchased from Charles River (Yokohama, Japan). Aged C57BL/6 mice were obtained from the National Institute on Aging. All animal procedures were approved by the University of Pennsylvania Institutional Animal Care and Use Committee and conformed to the National Institute of Health Guide for Care and Use of Laboratory Animals.

Stereotaxic Surgery

For olfactory bulb injections, mice anesthetized with Avertin (1.875% [w/v] 2,2,2-tribromoethanol, 1.25% [v/v] 3-methyl-1-butanol) received a unilateral stereotaxic injection of 0.5 μL of human α-Syn (h-α-Syn) PFFs in phosphate-buffered saline (PBS) (5 μg/μL) (n = 2), m-α-Syn PFFs in PBS (5 μg/μL) (n = 38), or PBS (n = 2) into the olfactory bulb (coordinates: −1.0 mm relative to the inferior cerebral vein or −4.5 mm relative to bregma; 0.9 mm from the midline; 1.5 mm beneath the scull surface) using a 33 gauge syringe. PFF- or PBS-injected mice were killed at indicated time points. Following perfusion with 4% (w/v) paraformaldehyde in PBS, the brains were removed and immersed in 4% (w/v) paraformaldehyde in PBS at 4°C overnight. Tissues were then embedded in paraffin for sectioning.

For dorsal striatum injections, stereotaxic surgery was performed as described previously with minor modifications (19). Mice anesthetized with ketamine-xylazine-acepromazine underwent stereotaxic injections using a 33-gauge syringe. Mice received a unilateral injection of 2.5 μL of m-α-Syn PFFs in PBS (2 μg/μL) (n = 6 for Fig. 5, n = 20 for Fig. 6) or PBS (n = 3 for Fig. 5) into the dorsal striatum (coordinates: 0.2 mm relative to bregma; 2.0 mm from midline; −3.2 mm beneath the skull surface). PFF- or PBS-injected mice were sacrificed at the indicated time points. Following perfusion with heparinized PBS, the brains were removed and immersed in 70% (v/v) ethanol (in 150 mM NaCl [pH 7.4]) at 4°C overnight. Tissues were then embedded in paraffin for sectioning.

Preparation of Recombinant Human and Mouse α-Syn Monomers and PFFs

For olfactory bulb injections, h-α-Syn and m-α-Syn were expressed in *Escherichia coli* BL21 (DE3) (BioDynamics Laboratory, Columbus, OH) and were purified as previously described in (28). Purified α-Syn was diluted in dialysis buffer (150 mM KCl, 50 mM Tris-HCl, pH 7.5) containing 0.1% (w/v) NaN3 to 7 mg/mL, followed by incubation at 37°C with constant agitation at 1000 rpm for 10 days. The characterization of resultant α-Syn PFFs was previously described in (28). The α-Syn PFF pellet was obtained by ultracentrifugation at 186 000g at 20°C for 20 minutes and stored at −80°C until use. The pellet was dissolved in 8 M guanidine hydrochloride to determine the protein concentration with a Pierce BCA Protein Assay kit (Thermo Fisher, Waltham, MA). The α-Syn PFFs in PBS (5 μg/μL) were sonicated with a Bioruptor bath sonicator (Diagenode, Denville, NJ) for 4 cycles (highest power, 30 seconds on, 30 seconds off at 4°C) before injections into the mouse olfactory bulb.

For dorsal striatum injections, m-α-Syn was expressed in BL21 (DE3) RIL cells and was purified as previously described in (29). Purified α-Syn was diluted in Dulbecco's PBS (pH 7.0; Mediatech, Holly Hill, FL) to 5 mg/mL, followed by incubation at 37°C with constant agitation at 1000 rpm for 7 days. The characterization of resultant α-Syn PFFs was previously described in (29). The solution was divided into aliquots and was stored at −80°C until use. The α-Syn PFFs were diluted to 2 μg/μL, followed by sonication with a Bioruptor bath sonicator for 10 cycles (highest power, 30 seconds on, 30 sec-

TABLE. Antibodies Used in This Study

Antibody	Epitope	Host Species	Dilution	Source
81A	α-Syn phosphorylated at Ser 129	Mouse monoclonal	1:20 000 (IHC), 1:5000 (IF)	(30)
#64	α-Syn phosphorylated at Ser 129	Mouse monoclonal	1:5000 (IHC), 1:1000 (IF)	Wako (Saitama, Japan, #015-25191)
EP1536Y	α-Syn phosphorylated at Ser 129	Rabbit monoclonal	1:20 000 (IHC), 1:5000 (IF)	Abcam (Cambridge, MA, #ab51253)
LB509	Human α-Syn	Mouse monoclonal	1:1000 (IHC)	Invitrogen (Carlsbad, CA, #180215)
Syn506	Misfolded α-Syn	Mouse monoclonal	1:5000 (IHC)	(31)
Syn514	Misfolded α-Syn	Mouse monoclonal	1:100 (IHC)	(31)
NeuN	Neuronal nuclear antigen	Mouse monoclonal	1:200 (IF)	Millipore (Burlington, MA, #MAB377)
GFAP	Glial fibrillary acidic protein	Mouse monoclonal	1:500 (IF)	Sigma (St. Louis, MO, #G3893)
Iba1	Ionized calcium-binding adapter molecule 1	Rabbit polyclonal	1:500 (IF)	Wako (#019-19741)
Olig2	Oligodendrocyte transcription factor 2	Rabbit polyclonal	1:500 (IF)	Millipore (#AB9610)
GST-pi	Glutathione S-transferase pi	Rabbit polyclonal	1:500 (IF)	MBL (Woburn, MA, #312)
PDGFR-α	Platelet-derived growth factor receptor-α	Rabbit monoclonal	1:200 (IF)	Cell Signaling (Danvers, MA, #3174S)
p62	Sequestosome 1 (p62/SQSTM1)	Rabbit polyclonal	1:1000 (IF)	MBL (#P045)
Ubiquitin	Ubiquitin	Rabbit polyclonal	1:500 (IF)	DAKO (Carpinteria, CA, #Z0458)
TPPP/p25	Tubulin polymerization promoting protein	Rabbit monoclonal	1:200 (IF)	Abcam (#ab92305)
pNF-H	Phosphorylated neurofilament heavy chain (pNF-H)	Mouse monoclonal	1:1000 (IF)	COVANCE (Princeton, NJ, #SMI31P)
MAP2	Microtubule-associated protein 2	Mouse monoclonal	1:200 (IF)	Millipore (#MAB3418)

Description of all antibodies used in this study, including epitopes they recognize, concentrations used, and how they were procured.
IF, immunofluorescence; IHC, immunohistochemistry.

onds off at 10°C) before injections into the mouse dorsal striatum.

Immunohistochemical Analysis

Eight- and 6-μm paraffin sections were prepared for the mice receiving olfactory bulb and dorsal striatum injections, respectively. Immunohistochemical analysis was performed as previously described in (28), and the primary antibodies used in this study are given in the Table. The sections were incubated at 4°C with primary antibodies for 2 days and then processed for visualization. As secondary antibodies, Histofine (Nichirei Bioscience, Tokyo, Japan) or biotinylated secondary antibodies (Vector laboratories, Burlingame, CA) were used for generating diaminobenzidine reaction product, and Alexa Fluor 488 or 594-conjugated antibodies (Molecular Probes, Eugene, OR) for immunofluorescence. For phosphorylated α-Syn (pSyn) and Thioflavin S ([ThS], Santa Cruz, Dallas, TX, #sc-391005) double-labeling staining, after immunolabeled with a pSyn antibody (81A), slides were incubated with 0.05% ThS in 50% ethanol followed by differentiation with 80% ethanol.

For the mice receiving olfactory bulb injections, every tenth paraffin section throughout the mouse brains was stained with a pSyn antibody (EP1536Y). To assess pSyn-positive neurons and glia in the ipsilateral anterior olfactory nucleus (AON), ipsilateral piriform cortex, anterior commissure, and ipsilateral fimbria, the numbers of neurons and glia with pSyn-positive aggregates were manually counted in each brain area of the coronal sections at 2.10, 0.26, 0.26, and −1.58 mm relative to bregma, respectively. Semiquantitative analyses were performed for neuronal α-Syn pathology on the 9 coronal sections (4.28, 2.80, 2.10, 1.78, 0.26, −1.58, −2.92, −4.04, and −5.34 mm relative to bregma), and color coded onto heat maps. The extent of EP1536Y-positive neuronal α-Syn

aggregates was graded as 0–3 (0, no pathology; 0.5, mild; 1, moderate; 2, severe; 3, very severe) based on the criteria reported previously (4). Scores were averaged between mice for each group (n = 3). Glial α-Syn pathology was manually counted for each coronal section and averaged across all mice in each group, then depicted schematically on the heat maps as purple dots (1 dot per 5 pSyn-positive glia). Quantification of EP1536Y-positive area of each glial cell was conducted with the ImageJ software (https://imagej.nih.gov/ij/). To assess neurons in the AON, the number of neuronal nuclear antigen (NeuN)-positive cells was counted in the coronal section at 2.34 mm relative to bregma using the ImageJ software.

For the mice receiving dorsal striatum injections, coronal sections at 0.14 mm relative to bregma were stained with a pSyn antibody (EP1536Y). The numbers of pSyn-positive neurons in the contralateral cingulate and motor cortices and pSyn-positive glia in the corpus callosum were manually counted.

Sections were examined with a BX43 microscope (Olympus, Tokyo, Japan), a BZ-x710 fluorescence microscope (KEYENCE, Osaka, Japan), an Eclipse Ni microscope (Nikon, Tokyo, Japan), and an FV-1000 confocal laser scanning microscope (Olympus).

Statistical Analysis

For comparison of 2 groups, a two-tailed unpaired Student t-test was performed. An F-test was performed to evaluate the differences in variances. For comparison of 3 or more groups, one-way ANOVA with Tukey's post hoc test was performed. A Brown-Forsythe test was performed to evaluate the differences in variances. Differences with p values of less than 0.05 were considered significant. Statistical calculations were performed with GraphPad Prism Software (GraphPad, San Diego, CA), Version 7.04.

879
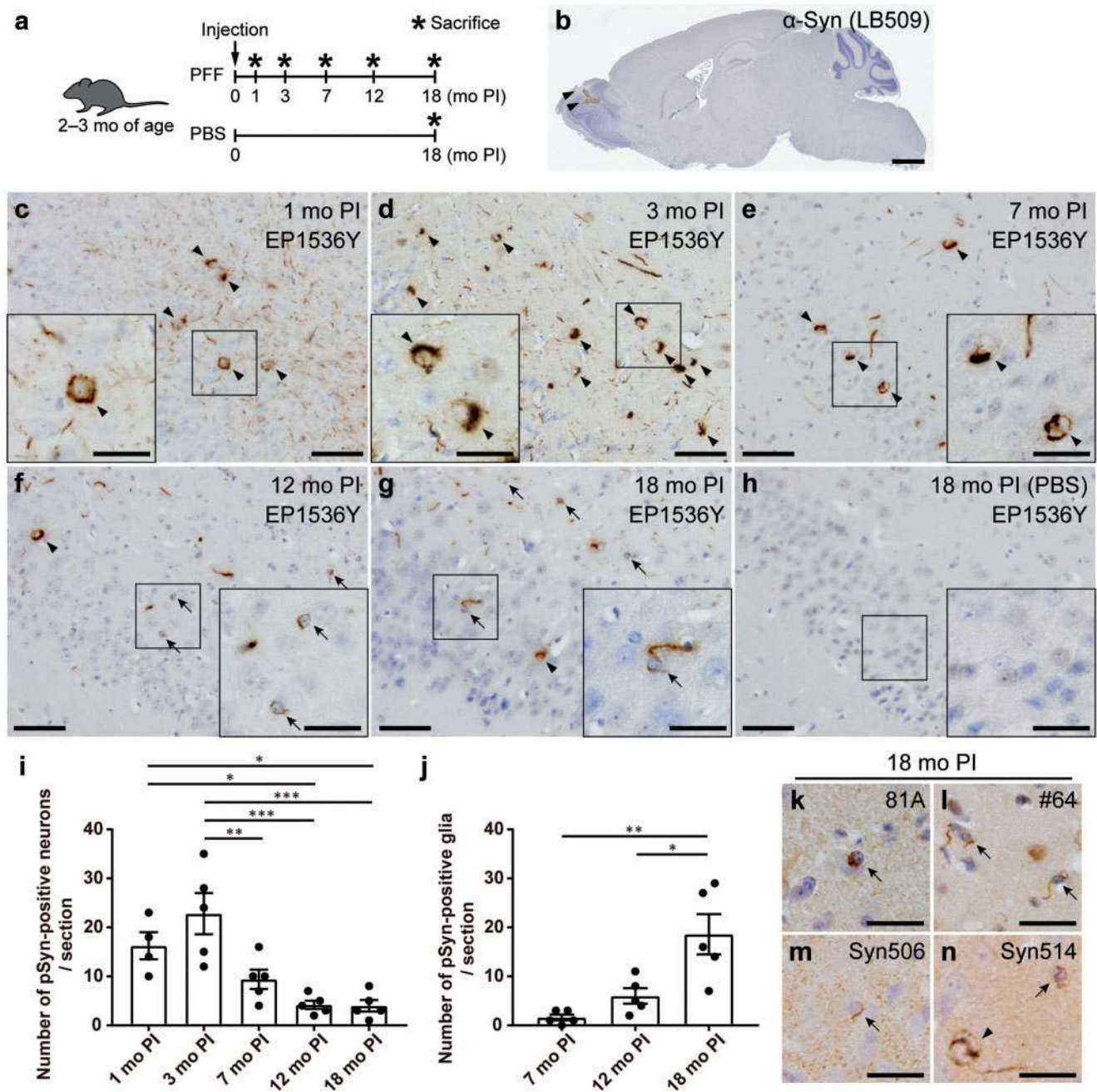
FIGURE 1. Progressive glial alpha-synuclein (α-Syn) pathology in the ipsilateral piriform cortex of the mice injected with mouse α-Syn (m-α-Syn) preformed fibrils (PFFs) into the olfactory bulb. **(A)** Schematic representation of experimental design. **(B)** The injection site shown by α-Syn immunohistochemistry (LB509) 3 hours after injections of h-α-Syn PFFs into the olfactory bulb (arrowheads). **(C–H)** Phosphorylated α-Syn (pSyn) immunohistochemistry (EP1536Y) in the ipsilateral piriform cortex of the mice injected with m-α-Syn PFFs or phosphate-buffered saline (PBS) into the olfactory bulb. Neuronal and glial pSyn pathology (arrowheads and arrows, respectively). No pSyn pathology was seen in mice injected with PBS **(H)**. **(I)** Quantification of the number of neurons with EP1536Y-positive pSyn pathology in the ipsilateral piriform cortex of the mice injected with m-α-Syn PFFs (1-month postinjection [PI], n = 4; 3, 7, 12, and 18-month PI, n = 5). One-way ANOVA with Tukey's multiple-comparisons test was performed; *$p < 0.05$, **$p < 0.01$, ***$p < 0.001$. Data are the mean ± SEM. **(J)** Quantification of the number of glia with EP1536Y-positive pSyn pathology in the ipsilateral piriform cortex of the mice injected with m-α-Syn PFFs (n = 5). One-way ANOVA with Tukey's multiple-comparisons test was performed; *$p < 0.05$, **$p < 0.01$. Data are the mean ± SEM. **(K–N)** Immunohistochemistry assessing pSyn (81A and #64) or misfolded α-Syn (Syn506 and Syn514) shows pSyn-positive or misfolded α-Syn-positive neurons and glia (arrowheads and arrows, respectively) at 18 months after injections of m-α-Syn PFFs. Scale bars: 1 mm **(A)**, 50 μm **(C–H)**, 20 μm **(C–H** insets, **K–N)**.

RESULTS

Progressive Glial α-Syn Pathology in the Regions Directly Connected to the PFF Injection Site in WT Mice

First, we analyzed the pathological change of the mice injected with m-α-Syn PFFs or PBS into the olfactory bulb (Fig. 1A). To confirm the successful injection into the olfactory bulb, we injected h-α-Syn PFFs into the olfactory bulb and then conducted immunohistochemistry at 3 hours postinjection (PI) using a h-α-Syn-specific antibody LB509 (Fig. 1B). We mainly used the pSyn antibody EP1536Y to detect pathological α-Syn aggregates throughout this study because the higher sensitivity and specificity of EP1536Y compared with other pSyn antibodies on the PFF-injected rodent brains were reported previously (32). At 1 month after injections of m-α-Syn PFFs into the olfactory bulb of C57BL/6J male mice, pSyn-positive pathology was observed mainly along the olfactory tract such as the AON, piriform cortex, amygdala, and entorhinal cortex (Fig. 1C; Supplementary Data Figs. S1A and S6). We first focused on the piriform cortex, which is one of the primary olfactory cortical areas and has reciprocal connections with the olfactory bulb (33). A number of pSyn-positive neurons were observed in the ipsilateral piriform cortex at 1 and 3 months after injections of m-α-Syn PFFs, but the number of pSyn-positive neurons decreased from 7-month PI (Fig. 1C–G, I). In contrast, no pSyn-positive glia were observed at 1- or 3-month PI, and only minimal pSyn-positive glia were observed at 7-month PI (Fig. 1C–E, J). However, pSyn-positive glia were clearly observed at 12-month PI and further increased in number at 18-month PI (Fig. 1F, G, J). Glial pathology was also detected by other pSyn antibodies and antibodies against misfolded α-Syn although this pathology was less sensitively detected by a pSyn antibody 81A and antibodies against misfolded α-Syn (Fig. 1K–N). Double immunofluorescence revealed that EP1536Y-positive neuronal and glial pathology were also positive for these antibodies (Supplementary Data Fig. S2). pSyn-positive neurons or glia were never observed in the mice injected with PBS (Fig. 1H).

We also chronologically analyzed the pathology in the AON, which has also reciprocal connection with the olfactory bulb (33). Similar to the pathological change in the ipsilateral piriform cortex, a considerable number of pSyn-positive neurons were observed in the ipsilateral AON at 1 and 3 months after injections of m-α-Syn PFFs, but the number of pSyn-positive neurons decreased from 7-month PI (Supplementary Data Fig. S1A–E, G). No pSyn-positive glia were observed at 1- or 3-month PI, and only minimal pSyn-positive glia were observed at 7-month PI (Supplementary Data Fig. S1A–C, H). However, pSyn-positive glia were clearly observed at 12-month PI and significantly increased in number at 18-month PI (Supplementary Data Fig. S1D, E, H). pSyn-positive neurons or glia were never observed in the mice injected with PBS (Supplementary Data Fig. S1F).

To examine whether the decrease in the number of pSyn-positive neurons was due to neuronal death, we counted the number of NeuN-positive neurons in the bilateral AON at 3- and 12-month PI (Supplementary Data Fig. S1I–M). When

compared with the contralateral AON, in which only a few pSyn-positive neurons were observed at both time points, the number of NeuN-positive neurons in the ipsilateral AON was significantly decreased at 12-month PI. This result is consistent with a previous study, suggesting that the decrease in the number of pSyn-positive neurons may be ascribed to neuronal death (34).

Collectively, only neuronal α-Syn aggregates were observed in the regions directly connected to the PFF injection site at 1 and 3 months after injections of m-α-Syn PFFs into the olfactory bulb of WT mice. They decreased in number from 7-month PI, while glial α-Syn aggregates appeared at 7-month PI and increased in number over time.

### α-Syn Pathology Is Observed Mostly in Neurons and Mature Oligodendrocytes

We analyzed the cell types of pSyn-positive cells in the ipsilateral piriform cortex at 18 months after injections of m-α-Syn PFFs into the olfactory bulb. As expected, pSyn-positive pathology was observed in NeuN-positive neurons (Fig. 2A). However, unexpectedly, a considerable number of pSyn-positive aggregates were observed in Olig2- or glutathione S-transferase pi (GST-pi)-positive mature oligodendrocytes (Fig. 2D, E, G, H). pSyn-positive pathology was rarely observed in glial fibrillary acidic protein (GFAP)-positive astrocytes, ionized calcium-binding adapter molecule 1 (Iba1)-positive microglia, or platelet-derived growth factor receptor α (PDGFRα)-positive oligodendrocyte precursor cells (OPCs) (Fig. 2B, C, F). We confirmed that pSyn-positive pathology was not observed in OPCs at 3- and 7-month PI to rule out the possibility that OPCs with pSyn-positive pathology differentiate into mature oligodendrocytes (Supplementary Data Fig. S3).

Abundant Oligodendroglial α-Syn Pathology in the White Matter Involved in the Neural Circuit of α-Syn Spreading

Next, we focused on the anterior commissure, whose major axons originate from the AON, piriform cortex, and amygdala and terminate in the contralateral olfactory bulb, AON, and piriform cortex (35). Only pSyn-positive fibers outside glial somata were observed in the anterior commissure at 1 month after injections of m-α-Syn PFFs, and pSyn-positive fibers with negligible pSyn-positive glia were observed at 3-month PI (Fig. 3A, B). However, pSyn-positive glia were clearly observed at 7-month PI, and abundant pSyn-positive glia were observed at 12-month PI, further increasing in number at 18-month PI (Fig. 3C–E, G). Only Glia with thin pSyn-positive aggregates were observed at 7-month PI, but glia with dense aggregates increased in number over time (Fig. 3H, I). This glial pathology was also detected by another pSyn antibody #64 and antibodies against misfolded α-Syn (Fig. 3K–M). However, this glial pathology was less prominent when the sections were stained with the pSyn antibody 81A (Fig. 3J). pSyn-positive glia were never observed in the mice injected with PBS (Fig. 3F). We confirmed that almost all pSyn-positive glia were Olig2- or GST-pi-positive

881
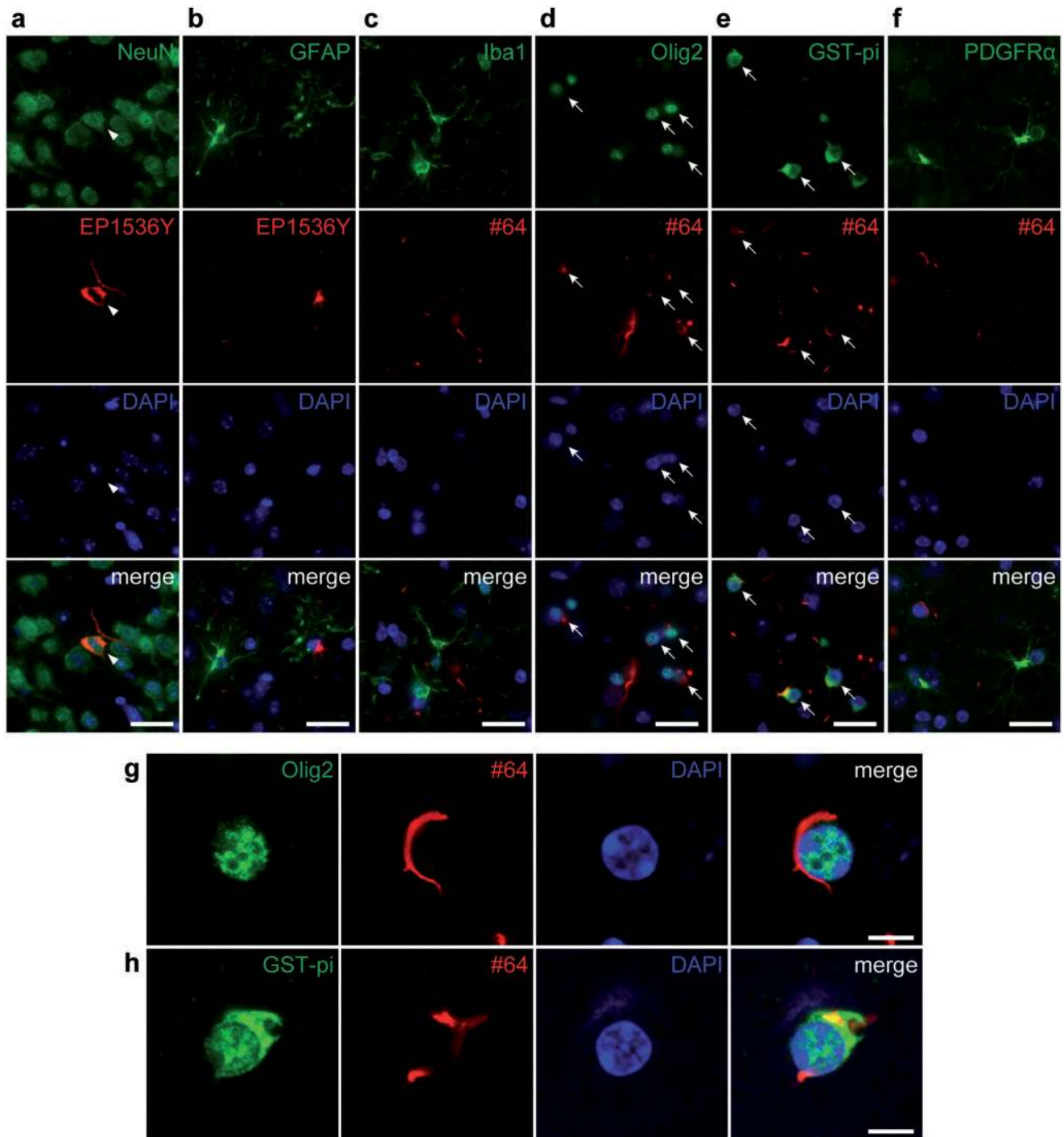
FIGURE 2. Alpha-synuclein pathology is observed mostly in neurons and mature oligodendrocytes in the ipsilateral piriform cortex at 18 months after injections of mouse α-Syn preformed fibrils into the olfactory bulb. Double label immunofluorescence images. **(A)** Neuronal nuclear antigen (NeuN) (green) and phosphorylated α-Syn (pSyn) (EP1536Y, red). pSyn-positive pathology in a NeuN-positive neuron (arrowheads). **(B)** Glial fibrillary acidic protein (green) and pSyn (EP1536Y, red). **(C)** Ionized calcium-binding adapter molecule 1 (green) and pSyn (#64, red). **(D)** Oligodendrocyte transcription factor 2 (Olig2) (green) and pSyn (#64, red). pSyn-positive pathology is seen in Olig2-positive oligodendrocytes (arrows). **(E)** Glutathione S-transferase pi (GST-pi) (green) and pSyn (#64, red). pSyn-positive pathology in GST-pi-positive mature oligodendrocytes (arrows). **(F)** Platelet-derived growth factor receptor α (green) and pSyn (#64, red). **(G)** Confocal microscope images of Olig2 (green) and pSyn (#64, red). **(H)** Confocal microscope images of GST-pi (green) and pSyn (#64, red). Scale bars: 20 μm **(A–F)**, 5 μm **(G, H)**.
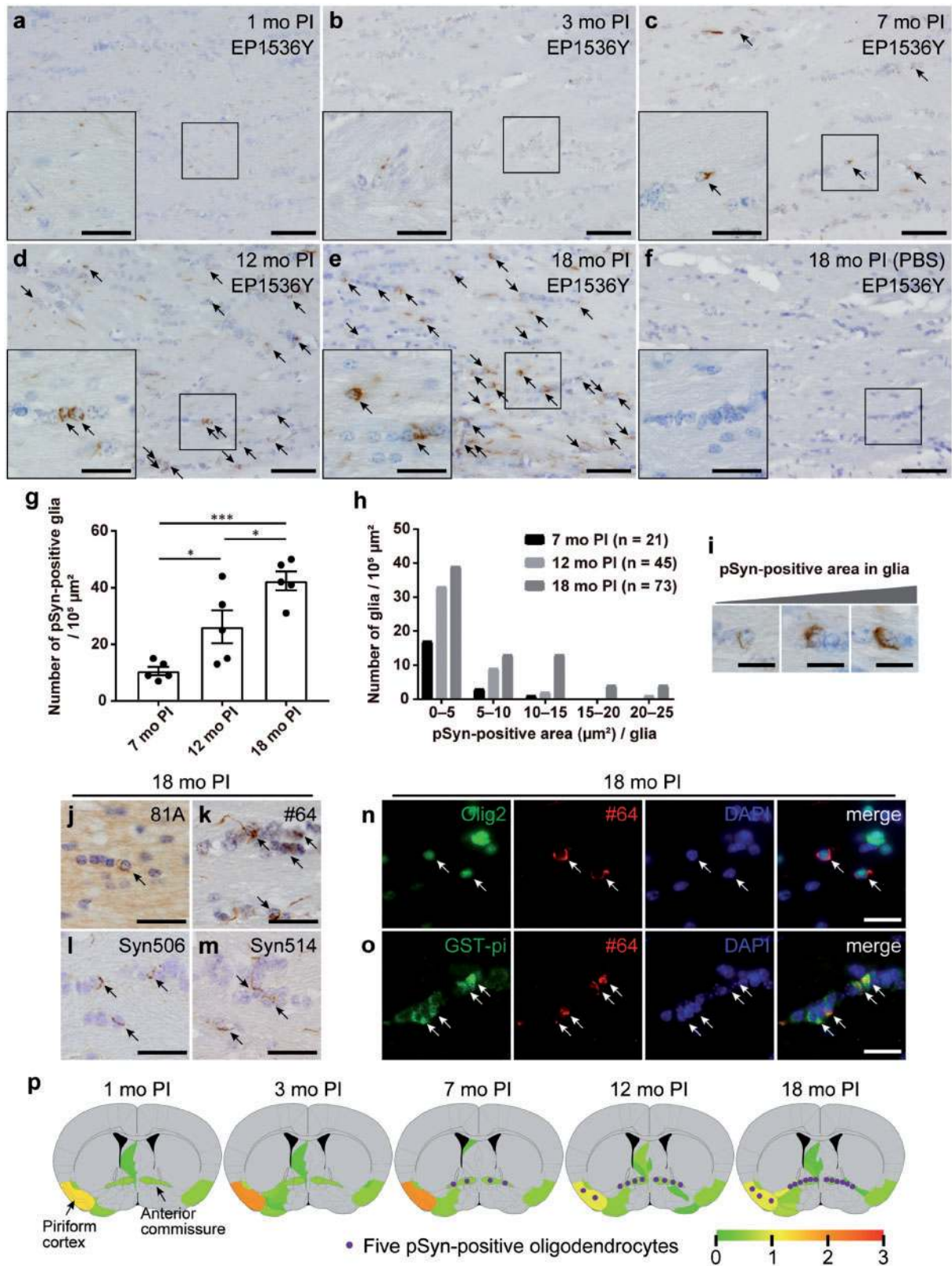
FIGURE 3. Progressive oligodendroglial alpha-synuclein (α-Syn) pathology in the anterior commissure of the mice injected with mouse α-Syn (m-α-Syn) preformed fibrils (PFFs) into the olfactory bulb. **(A–F)** Phosphorylated α-Syn (pSyn)

mature oligodendrocytes, and not GFAP-positive astrocytes, Iba1-positive microglia, or PDGFRα-positive OPCs (Supplementary Data Fig. S4b–d). We further confirmed that this pSyn-positive pathology was not positive for neurofilament, and there are almost no NeuN-positive neurons or microtubule-associated protein 2 (MAP2)-positive dendrites in the anterior commissure (Supplementary Data Fig. S4A, E, F).

We also chronologically analyzed the pathology in the fimbria, which is one of the major outputs from the hippocampus and is composed of the fibers of secondary or higher neurons from the olfactory bulb. Similar to the pathological change in the anterior commissure, only a few pSyn-positive fibers were observed in the ipsilateral fimbria at 1- and 3-month PI (Supplementary Data Fig. S5A, B). However, small numbers of pSyn-positive glia appeared at 7-month PI and increased in number over time (Supplementary Data Fig. S5C–E, G). We confirmed that almost all pSyn-positive glia were Olig2-positive oligodendrocytes by double immunofluorescence (data not shown). pSyn-positive glia were never observed in the mice injected with PBS (Supplementary Data Fig. S5F). The distribution of neuronal α-Syn pathology is summarized as heat maps with oligodendroglial α-Syn pathology as dots (Fig. 3P; Supplementary Data Fig. S6).

In summary, only pSyn-positive fibers were observed in the white matter involved in a neural circuit of α-Syn spreading at 1 and 3 months after injections of m-α-Syn PFFs. However, oligodendroglial α-Syn pathology appeared at 7-month PI and became abundant at later time points. Oligodendroglial α-Syn aggregates gradually grew in size and number over time.

α-Syn Pathology in Oligodendrocytes Exhibits the Pathological Characteristics of GCIs

Next, we examined the pathological characteristics of the oligodendroglial α-Syn pathology in the anterior commissure of the mice injected with m-α-Syn PFFs into the olfactory bulb. Most of pSyn-positive oligodendroglial pathology was also immunopositive for p62 and ubiquitin, both of which are also positive in GCIs (Fig. 4A, B) (36, 37). Some oligodendroglial pSyn-positive pathology was also positive for ThS, indicating that they were composed of β-sheet-rich amyloid fibrils (Fig. 4C). Tubulin polymerization promoting protein (TPPP/p25) has been reported to accumulate in GCIs (38), and some pSyn-positive oligodendroglial pathology colocalized with TPPP/p25 accumulations in PFF-injected mice while neither pSyn-positive oligodendroglial pathology nor TPPP/p25 accumulation was observed in PBS-injected mice (Fig. 4D, E). All these observations indicate that oligodendroglial α-Syn pathology in the mice injected with m-α-Syn PFFs share properties in common with GCIs.

Abundant Oligodendroglial α-Syn Pathology in Another Fibril-Induced Mouse Model of Synucleinopathy

To investigate whether the phenomenon of oligodendroglial α-Syn aggregation after long PI intervals is common among fibril-injected mouse models, we analyzed the pathology of the B6C3 female mice injected with m-α-Syn PFFs into the dorsal striatum as an independent experiment (Fig. 5A). We first examined the pathology in the contralateral cingulate and motor cortices of this model based on our previous report (17). Only neuronal α-Syn pathology was observed at 3-month PI, while less neuronal α-Syn pathology and a considerable amount of glial α-Syn pathology was observed at 24-month PI (Fig. 5B, C). We confirmed that almost all pSyn-positive glia were Olig2-positive oligodendrocytes by double immunofluorescence (Fig. 5D). We next examined the pathology in the corpus callosum, the white matter. Only pSyn-positive fibers were observed at 3-month PI, while abundant glial α-Syn pathology was observed at 24-month PI (Fig. 5E, F). Again, double immunofluorescence revealed that almost all pSyn-positive glia were Olig2-positive oligodendrocytes

FIGURE 3. Continued
immunohistochemistry (EP1536Y) in the anterior commissure. Note glial pSyn pathology (arrows in **C–E**). No pSyn pathology is seen in the mice injected with phosphate-buffered saline **(F)**. **(G)** Quantification of the number of glia with EP1536Y-positive pSyn pathology in the anterior commissure of the mice injected with m-α-Syn PFFs (n = 5). One-way ANOVA with Tukey's multiple-comparisons test was performed; *p < 0.05, ***p < 0.001. Data are the mean ± SEM. **(H)** Distribution of pSyn (EP1536Y)-positive area of each glial cell at 7, 12, and 18 months after injections of m-α-Syn PFFs. **(I)** Representative images of glia with small to large EP1536Y-positive pSyn aggregates. **(J–M)** Immunohistochemistry assessing pSyn (81A and #64) or misfolded α-Syn (Syn506 and Syn514) shows pSyn-positive or misfolded α-Syn-positive glia (arrows) at 18 months after injections of m-α-Syn PFFs. **(N)** Double immunofluorescence staining for oligodendrocyte transcription factor 2 (Olig2) (green) and pSyn (#64, red). pSyn-positive pathology in Olig2-positive oligodendrocytes (arrows). **(O)** Double immunofluorescence for glutathione S-transferase pi (GST-pi) (green) and pSyn (#64, red). pSyn-positive pathology in GST-pi-positive mature oligodendrocytes (arrows). **(P)** Semiquantitative analysis of α-Syn pathology based on pSyn immunohistochemistry (EP1536Y) at 1-, 3-, 7-, 12-, and 18-month postinjection. Representative coronal planes (0.26 mm relative to bregma) containing the piriform cortex and anterior commissure are shown here, and 8 additional coronal planes at 4.28, 2.80, 2.10, 1.78, −1.58, −2.92, −4.04, and −5.34 mm relative to bregma are shown in Supplementary Data Figure S6. Left is the injection side. Heat map colors represent the extent of neuronal α-Syn pathology (gray [0], no pathology; red [3], maximum pathology). Scores were averaged among mice for each group (n = 3). Oligodendroglial α-Syn aggregates were counted and averaged across all mice in each group, then depicted schematically on the heat maps as purple dots (1 dot per 5 pSyn-positive oligodendrocytes). Scale bars: 50 μm **(A–F)**, 20 μm **(A–F** insets, **J–O)**, 10 μm **(I)**.
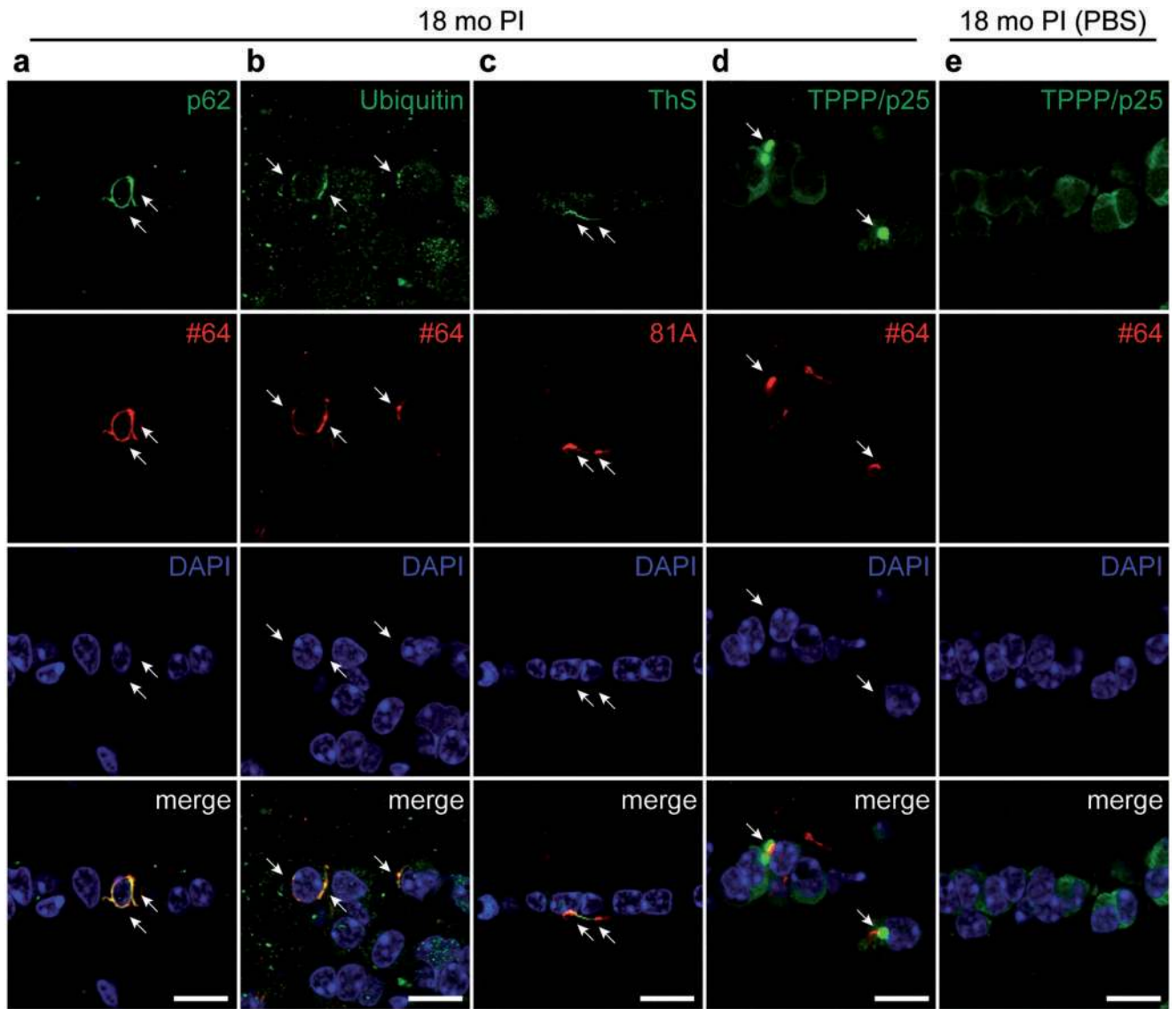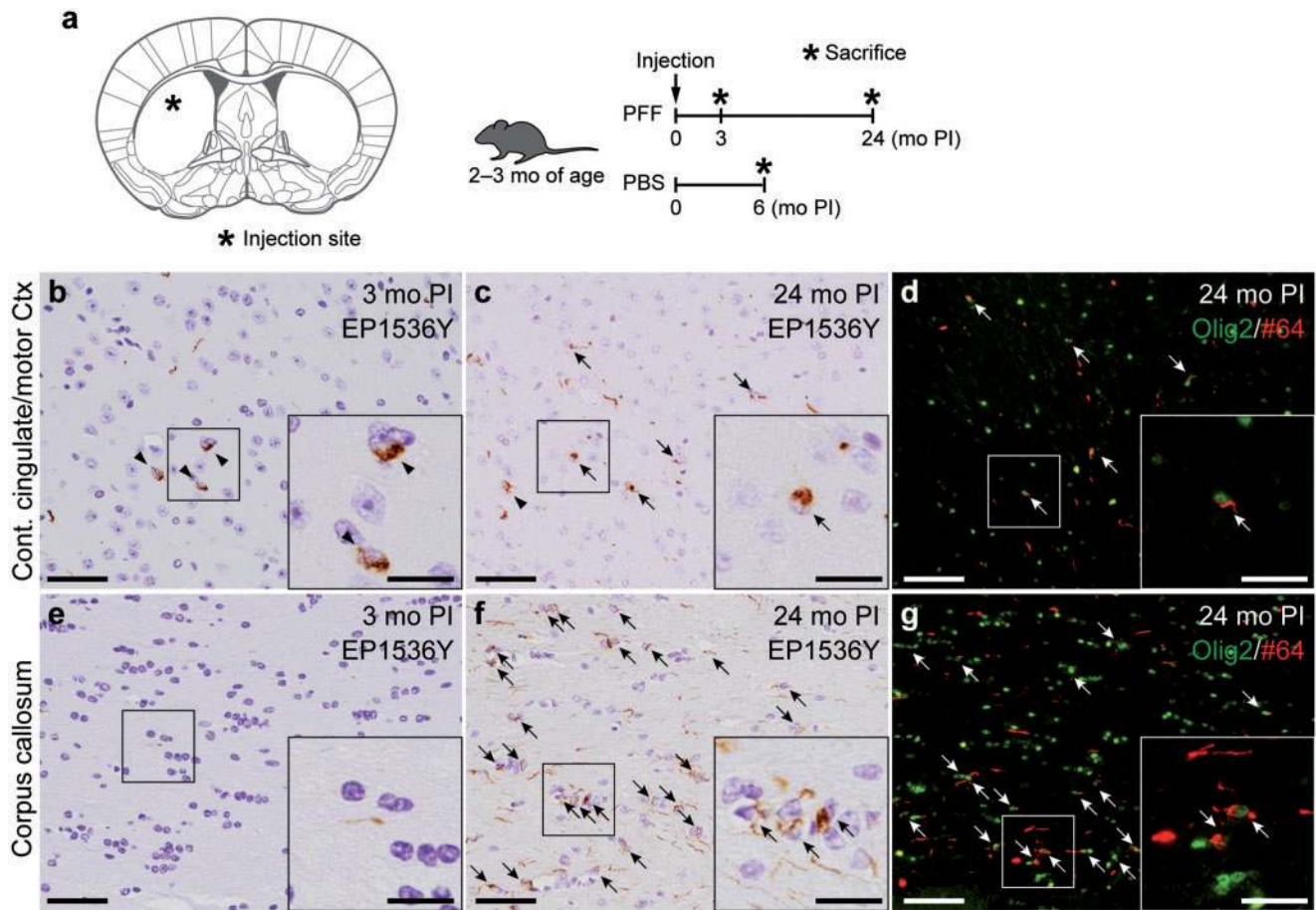
FIGURE 4. Alpha-synuclein pathology in oligodendrocytes exhibits the pathological characteristics of GCIs. Confocal double immunofluorescence microscopic images of the anterior commissure at 18 months after injections of mouse α-Syn preformed fibrils **(A–D)** or phosphate-buffered saline **(E)** into the olfactory bulb. **(A)** p62 (green) and phosphorylated α-Syn (pSyn) (#64, red). pSyn-positive pathology colocalizes with p62 (arrows). **(B)** Ubiquitin (green) and pSyn (#64, red). pSyn-positive pathology colocalizes with ubiquitin (arrows). **(C)** Thioflavin S (ThS, green) and pSyn (#64, red). pSyn-positive pathology colocalizes with ThS (arrows). **(D, E)** Tubulin polymerization-promoting protein (TPPP/p25, green) and pSyn (#64, red). Part of pSyn-positive pathology colocalizes with TPPP/p25 accumulation (arrows) **(D)**. Scale bars: 20 μm.

(Fig. 5G). pSyn-positive pathology was never observed in the mice injected with PBS (data not shown).

Taken together, we confirmed that another mouse model injected with m-α-Syn PFFs also exhibited neuronal α-Syn pathology after short PI intervals and oligodendroglial α-Syn pathology after longer PI intervals in the brains. This indicates that the formation of oligodendroglial α-Syn pathology is independent of injection site and mouse background, and at least m-α-Syn PFFs generated in two different ways induce the same phenomenon.

PI Intervals Rather Than Aging Correlate With Oligodendroglial α-Syn Aggregation

The results indicate that longer PI intervals are required for young mice injected with m-α-Syn PFFs to form oligodendroglial α-Syn aggregates in their brains compared with neuronal α-Syn aggregates. To address whether the onset of oligodendroglial pathology is the result of an extended PI interval or is facilitated by aging, we examined the pathology of young and aged mice injected with m-α-Syn PFFs into the dorsal striatum at 3- and 6-month PI (Fig. 6A). We evaluated

885

FIGURE 5. Oligodendroglial alpha-synuclein pathology in another preformed fibril-injected mouse model of synucleinopathy. **(A)** Left panel: schematic showing the dorsal striatum injection site in this mouse model (0.26 mm relative to bregma). Right panel: Schematic representation of experimental design. **(B**, **C**, **E**, **F)** Phosphorylated α-Syn (pSyn) immunohistochemistry (EP1536Y) in the contralateral cingulate and motor cortices **(B**, **C)** and in the corpus callosum **(E**, **F)** at 0.14 mm relative to bregma. **(D**, **G)** Double label immunofluorescence images of the contralateral cingulate and motor cortices **(D)** and corpus callosum **(G)**. Oligodendrocyte transcription factor 2 (green) and pSyn (#64, red). Neuronal and glial pSyn pathology (arrowheads and arrows, respectively). Scale bars: 50 μm **(B–G)**, 20 μm **(B–G** insets).

neuronal pathology in the contralateral cingulate and motor cortices and oligodendroglial pathology in the corpus callosum (Fig. 6B–K). Unexpectedly, fewer neuronal α-Syn aggregates were observed in the contralateral cingulate and motor cortices of aged mice compared with the young mice at both time points, albeit not reaching statistical significance at 3-month PI (Fig. 6J). Although only minimal oligodendroglial α-Syn aggregates were observed in the corpus callosum at 3-month PI, oligodendroglial α-Syn aggregates clearly appeared at 6-month PI in both the young and aged mice. However, again, fewer oligodendroglial α-Syn aggregates were observed at 6-month PI in the aged mice compared with the young mice (Fig. 6K).

These results indicate that aging does not augment the overall abundance of neuronal or oligodendroglial α-Syn pathology. PI intervals, not aging, correlate with oligodendroglial α-Syn aggregation.

DISCUSSION

Oligodendroglial α-Syn pathology resembling one seen in human synucleinopathies had not been reported previously in animals injected with PFFs (19–21, 23, 34, 39) except transgenic mice injected with PFFs (25, 40). In this study, long-term observations revealed a slow progressive accumulation of oligodendroglial α-Syn pathology in WT mice injected with m-α-Syn PFFs.

To explain heterogeneity of neurodegenerative diseases sharing the same pathological protein, the "strain hypothesis" has drawn considerable attention (17, 18, 41). A previous study demonstrated that injections of another α-Syn strain termed "ribbons," but not "fibrils," into the rat brains in combination with virally mediated overexpression of α-Syn induces oligodendroglial α-Syn pathology, thereby raising the possibility that pathological heterogeneity of α-Syn in diverse synucleinopathies is derived from distinct strains (42). In
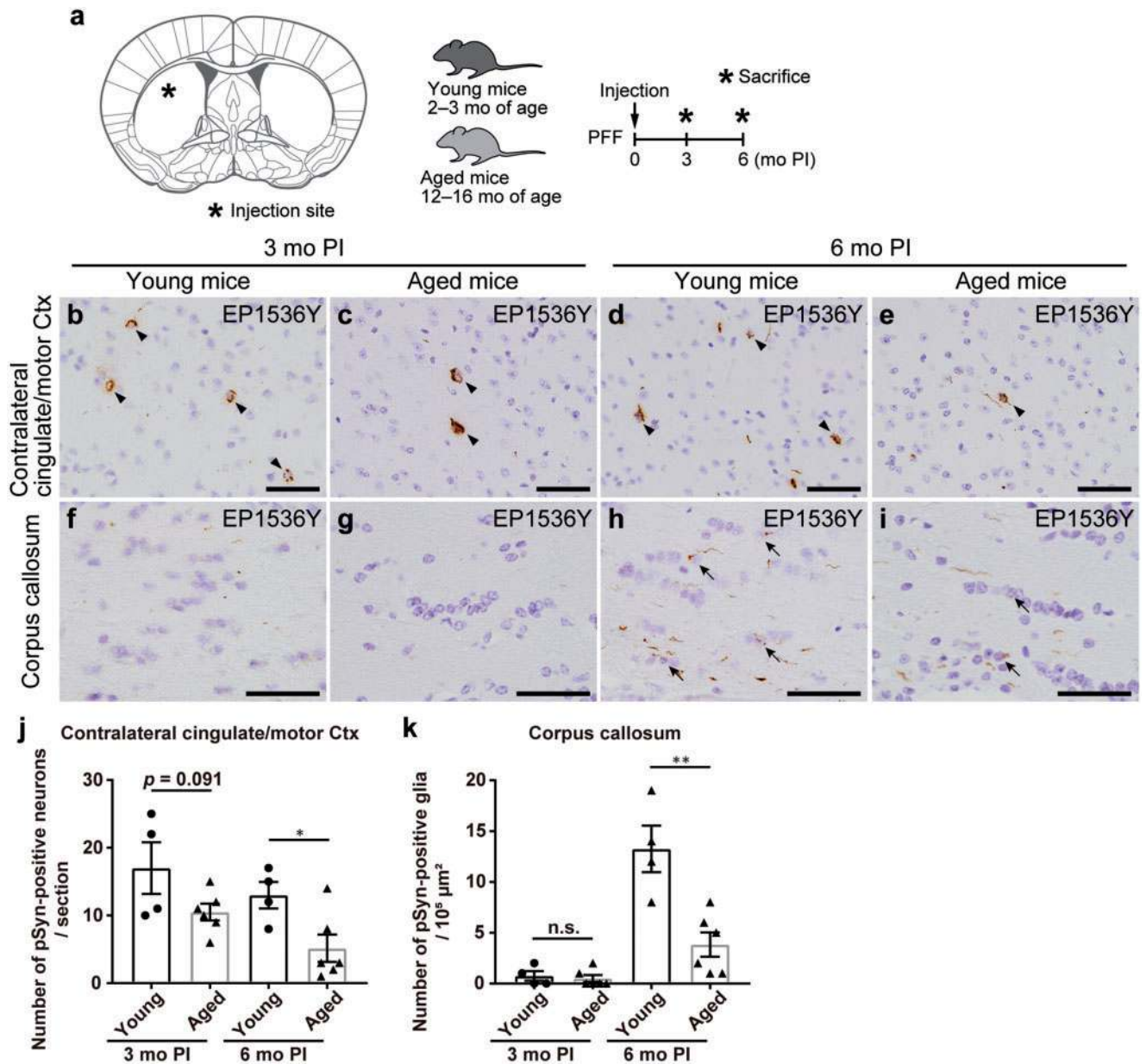
FIGURE 6. Postinjection (PI) intervals rather than aging correlate with oligodendroglial alpha-synuclein aggregation. **(A)** Left panel: Schematic showing the dorsal striatum injection site in this mouse model (0.26 mm relative to bregma). Right panel: Schematic representation of experimental design. **(B–I)** Phosphorylated α-Syn (pSyn) immunohistochemistry (EP1536Y) at 0.14 mm relative to bregma. Contralateral cingulate and motor cortices **(B–E)**, corpus callosum **(F–I)**. Neuronal and glial pSyn pathology (arrowheads and arrows, respectively). **(J, K)** Quantification of the number of neurons or glia with EP1536Y-positive pSyn pathology in the contralateral cingulate and motor cortices, and corpus callosum (3- and 6-month PI in young mice, n = 4; 3- and 6-month PI in aged mice, n = 6). A two-tailed unpaired Student t-test was performed; *p < 0.05, **p < 0.01, n.s., not significant. Data are the mean ± SEM. Scale bars: 50 μm **(B–I)**.

tauopathies, injections into mouse brains of brain lysates of patients with progressive supranuclear palsy (PSP) and corticobasal degeneration (CBD), but not those of patients with Alzheimer disease, replicates the glial pathology characteristic of PSP and CBD even at 1-month PI, suggesting that the diversity of tauopathies can be explained by tau strains (43, 44). We previously demonstrated that brain lysates of patients with

MSA have higher potency of inducing neuronal α-Syn pathology and show distinct transmission patterns in mouse brains compared with α-Syn PFFs and brain lysates of patients with PD (25). However, no oligodendroglial α-Syn pathology was detected up to 6-month PI in WT mice injected with brain lysates of patients with MSA (25). Based on the observations in this study, α-Syn aggregates form more slowly in

887
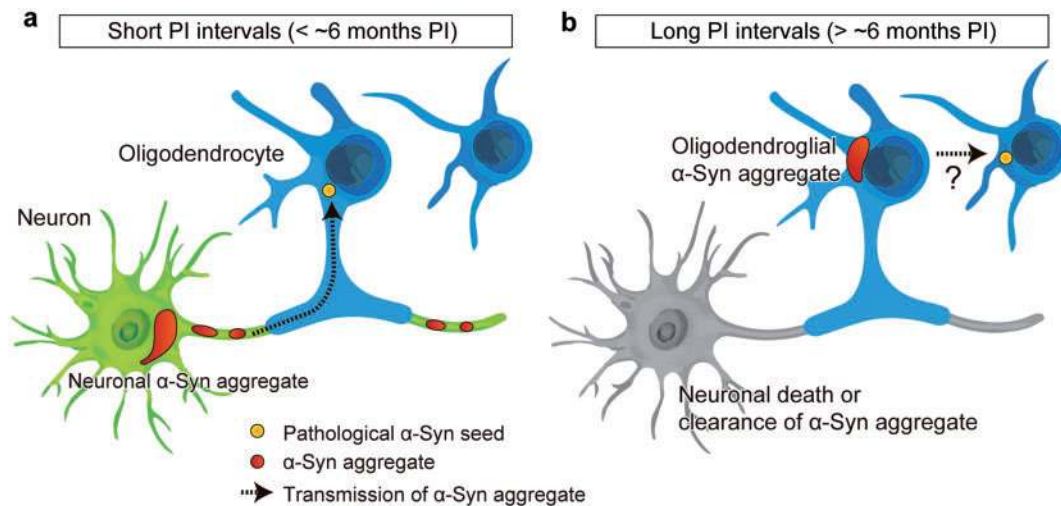
FIGURE 7. Proposed pathological mechanisms of neuronal and oligodendroglial alpha-synuclein (α-Syn) pathology in the mice injected with mouse α-Syn (m-α-Syn) preformed fibrils (PFFs). The mice injected with m-α-Syn PFFs develop phosphorylated α-Syn (pSyn)-positive neuronal aggregates after short postinjection (PI) intervals (less than ∼6 months PI as shown in panel **(A)**. Pathological α-Syn seeds presumably transmit from axons to oligodendrocytes, but pSyn-positive pathology is rarely seen in oligodendrocytes. After longer PI intervals (more than ∼6 months PI as shown in panel **(B)**, the majority of pSyn-positive neuronal aggregates disappear presumably because of neuronal death, although the possibility of clearance of α-Syn aggregates cannot be excluded. pSyn-positive oligodendroglial aggregates emerge and then increase in number over time. Pathological α-Syn seeds might transmit among oligodendrocytes.

oligodendrocytes than in neurons, so longer observation might be needed to reveal GCI-like pathology in the mice injected with brain lysates of patients with MSA.

Although it has received little attention, astroglial and oligodendroglial α-Syn pathology in PD and DLB has been reported (45–50). Oligodendroglial α-Syn aggregates in PD and DLB, sometimes called coiled bodies (47, 50), are morphologically different from GCIs in MSA. In this study, some of the oligodendroglial α-Syn aggregates observed in the mice injected with m-α-Syn PFFs resembled coiled bodies seen in PD and DLB. However, we do not argue that oligodendroglial α-Syn pathology observed in these mice is coiled body-like or GCI-like because the inoculum used in this study is m-α-Syn PFFs, but not brain lysates of patients with PD/DLB or MSA. Moreover, no markers have been reported to differentiate these two types of oligodendroglial pathology. Nonetheless, given that abundant oligodendroglial α-Syn pathology was observed in the white matter of m-α-Syn PFF-injected mice, we think that the observations in this study provide crucial clues for the pathological mechanisms of oligodendroglial α-Syn aggregation in MSA. Further studies are required to determine whether the pathological characteristics (e.g. affected cell types, morphology, and spread) depend on the α-Syn strains in the inoculum and/or on the host species. In other words, injections of other α-Syn strains or using other animal species such as nonhuman primates as a host may lead to distinct neuronal and glial α-Syn pathology.

We propose the hypothetical mechanisms for oligodendroglial α-Syn aggregation based on the observations in this study (Fig. 7). The possible pathological mechanisms described below are not mutually exclusive and may occur in parallel. First, α-Syn aggregates form very slowly in oligodendrocytes compared with those in neurons. Neuronal α-Syn aggregates were observed at 1 month after injections of m-α-Syn PFFs and decreased in number from 7-month PI. This decrease is presumably because of neuronal death (51), but the possibility of clearance of α-Syn aggregates cannot be excluded. In contrast, oligodendroglial α-Syn aggregates appeared at 7-month PI and increased in number over time. Since dense oligodendroglial α-Syn aggregates were observed at later time points, α-Syn aggregates seem to grow in size over time in oligodendrocytes. A previous study demonstrated α-Syn expression in cells of oligodendrocyte lineage using several in vitro models and oligodendroglial nuclei isolated by fluorescence-activated cell sorting from rodent and human brains (52). However, since the expression level of α-Syn is lower in oligodendrocytes than in neurons (53), templated recruitment of endogenous α-Syn may be delayed in oligodendrocytes. Consistent with this notion, it has been reported that templated recruitment of endogenous α-Syn occurs in primary rat oligodendrocytes in vitro and in oligodendrocytes of mouse brains in vivo (54).

Second, α-Syn aggregates may be transmitted through axons to oligodendrocytes. In this study, abundant oligodendroglial pathology was observed in the white matter of the mice injected with m-α-Syn PFFs. Considering that the white matter connects with the PFF injection site or the brain regions affected by α-Syn pathology exclusively via axons, these observations indicate that axon-to-oligodendrocyte transmission of α-Syn aggregates contributes to the formation of oligodendroglial α-Syn pathology. In this regard, it seems reasonable that α-Syn aggregates did not form in OPCs but

rather in mature oligodendrocytes that are in contact with axons through their myelin sheath. However, oligodendroglial α-Syn aggregates continued to increase in number up to 18-month PI despite the fact that only a few neuronal α-Syn aggregates were seen at later time points, which might argue against an exclusive role for axons in transmitting α-Syn pathology to oligodendrocytes. Based on these observations, we speculate that transmission of α-Syn aggregates among oligodendrocytes might also contribute to the progression of oligodendroglial α-Syn pathology. Further studies are required to verify these hypotheses.

Lastly, PI intervals rather than aging per se correlate with the initial formation of oligodendroglial α-Syn aggregates. Since aging is a common and strong risk factor for neurodegenerative diseases, we expected more α-Syn pathology in the aged mice compared with the young mice. For example, protein degradation systems, which are compromised by aging, play key roles in removing abnormal misfolded proteins (7, 55, 56). However, contrary to our expectations, fewer neuronal and oligodendroglial α-Syn aggregates were observed in aged mice compared with young mice. Since aging is associated with diverse physiological changes across different cell types (55), other mechanisms (e.g. α-Syn expression in neurons and oligodendrocytes, uptake of PFFs by neurons, and clearance of PFFs by glia) might affect the formation of α-Syn pathology in aged mice. In addition, we cannot exclude the possibility that faster cell loss of α-Syn aggregate-bearing neurons or oligodendrocytes occurs in aged mice, hence affecting the amount of α-Syn pathology detected.

The origin of α-Syn aggregates in MSA is still under debate. One possibility is that MSA is a primary oligodendrogliopathy and that oligodendroglial α-Syn pathology secondarily affects neurons (57–59). Another possibility is that MSA is a neuronal disease with secondary accumulation of α-Syn in oligodendrocytes (60–62). The observations in this study support the latter possibility. However, α-Syn aggregate-bearing oligodendrocytes may not be just a by-product of the disease process, but may also induce inflammation and reduce trophic support for neurons, further exacerbating neurodegeneration (58). Moreover, we recently demonstrated that oligodendrocytes transform misfolded h-α-Syn into a distinct strain that is highly potent in seeding α-Syn aggregation, suggesting that oligodendroglial α-Syn aggregates may further accelerate the disease progression (25). Further studies are required to determine how oligodendroglial α-Syn aggregates contribute to pathological progress and to its consequence, clinical symptoms in MSA. For example, injections of m-α-Syn PFFs into neuron-specific α-Syn conditional knockout mice may allow us to investigate the role of oligodendroglial α-Syn aggregates on disease progress.

In conclusion, this study provides evidence that oligodendroglial α-Syn pathology can be replicated even in WT mice and provides novel insights into the pathological mechanisms of oligodendroglial α-Syn aggregation in MSA. Although almost no effective treatment is available for MSA today, further elucidation of these pathological mechanisms could pave the way for new therapeutic targets of MSA.

REFERENCES

1. Spillantini MG, Schmidt ML, Lee VM, et al. Alpha-synuclein in Lewy bodies. Nature 1997;388:839–40
2. Tu PH, Galvin JE, Baba M, et al. Glial cytoplasmic inclusions in white matter oligodendrocytes of multiple system atrophy brains contain insoluble alpha-synuclein. Ann Neurol 1998;44:415–22
3. Lippa CF, Duda JE, Grossman M, et al. DLB and PDD boundary issues: Diagnosis, treatment, molecular pathology, and biomarkers. Neurology 2007;68:812–9
4. McKeith IG, Dickson DW, Lowe J, et al. Diagnosis and management of dementia with Lewy bodies: Third report of the DLB consortium. Neurology 2005;65:1863–72
5. Krismer F, Wenning GK. Multiple system atrophy: Insights into a rare and debilitating movement disorder. Nat Rev Neurol 2017;13:232–43
6. Lee VM, Trojanowski JQ. Mechanisms of Parkinson's disease linked to pathological alpha-synuclein: New targets for drug discovery. Neuron 2006;52:33–8
7. Ebrahimi-Fakhari D, Wahlster L, McLean PJ. Protein degradation pathways in Parkinson's disease: Curse or blessing. Acta Neuropathol 2012; 124:153–72
8. Yazawa I, Giasson BI, Sasaki R, et al. Mouse model of multiple system atrophy alpha-synuclein expression in oligodendrocytes causes glial and neuronal degeneration. Neuron 2005;45:847–59
9. Shults CW, Rockenstein E, Crews L, et al. Neurological and neurodegenerative alterations in a transgenic mouse model expressing human alpha-synuclein under oligodendrocyte promoter: Implications for multiple system atrophy. J Neurosci 2005;25:10689–99
10. Kahle PJ, Neumann M, Ozmen L, et al. Hyperphosphorylation and insolubility of alpha-synuclein in transgenic mouse oligodendrocytes. EMBO Rep 2002;3:583–8
11. Langerveld AJ, Mihalko D, DeLong C, et al. Gene expression changes in postmortem tissue from the rostral pons of multiple system atrophy patients. Mov Disord 2007;22:766–77
12. Miller DW, Johnson JM, Solano SM, et al. Absence of alpha-synuclein mRNA expression in normal and multiple system atrophy oligodendroglia. J Neural Transm 2005;112:1613–24
13. Asi YT, Simpson JE, Heath PR, et al. Alpha-synuclein mRNA expression in oligodendrocytes in MSA. Glia 2014;62:964–70
14. The Multiple-System Atrophy Research Collaboration. Mutations in COQ2 in familial and sporadic multiple-system atrophy. N Engl J Med 2013;369:233–44
15. Vilarino-Guell C, Soto-Ortolaza AI, Rajput A, et al. MAPT H1 haplotype is a risk factor for essential tremor and multiple system atrophy. Neurology 2011;76:670–2
16. Mitsui J, Matsukawa T, Sasaki H, et al. Variants associated with Gaucher disease in multiple system atrophy. Ann Clin Transl Neurol 2015;2:417–26
17. Peng C, Gathagan RJ, Lee VM. Distinct alpha-synuclein strains and implications for heterogeneity among alpha-synucleinopathies. Neurobiol Dis 2018;109:209–18
18. Jucker M, Walker LC. Propagation and spread of pathogenic protein assemblies in neurodegenerative diseases. Nat Neurosci 2018;21:1341–9
19. Luk KC, Kehm V, Carroll J, et al. Pathological alpha-synuclein transmission initiates Parkinson-like neurodegeneration in nontransgenic mice. Science 2012;338:949–53
20. Masuda-Suzukake M, Nonaka T, Hosokawa M, et al. Prion-like spreading of pathological alpha-synuclein in brain. Brain 2013;136:1128–38
21. Paumier KL, Luk KC, Manfredsson FP, et al. Intrastriatal injection of pre-formed mouse alpha-synuclein fibrils into rats triggers alpha-synuclein pathology and bilateral nigrostriatal degeneration. Neurobiol Dis 2015;82:185–99
22. Recasens A, Dehay B, Bove J, et al. Lewy body extracts from Parkinson disease brains trigger alpha-synuclein pathology and neurodegeneration in mice and monkeys. Ann Neurol 2014;75:351–62

23. Shimozawa A, Ono M, Takahara D, et al. Propagation of pathological alpha-synuclein in marmoset brain. Acta Neuropathol Commun 2017; 5:12

24. Prusiner SB, Woerman AL, Mordes DA, et al. Evidence for alpha-synuclein prions causing multiple system atrophy in humans with parkinsonism. Proc Natl Acad Sci USA 2015;112:E5308–17

25. Peng C, Gathagan RJ, Covell DJ, et al. Cellular milieu imparts distinct pathological alpha-synuclein strains in alpha-synucleinopathies. Nature 2018;557:558–63

26. Bernis ME, Babila JT, Breid S, et al. Prion-like propagation of human brain-derived alpha-synuclein in transgenic mice expressing human wild-type alpha-synuclein. Acta Neuropathol Commun 2015;3:75

27. Flurkey K, Currer JM. Pitfalls of animal model systems in ageing research. Best Pract Res Clin Endocrinol Metab 2004;18:407–21

28. Uemura N, Yagi H, Uemura MT, et al. Inoculation of alpha-synuclein preformed fibrils into the mouse gastrointestinal tract induces Lewy body-like aggregates in the brainstem via the vagus nerve. Mol Neurodegen 2018;13:21

29. Luk KC, Covell DJ, Kehm VM, et al. Molecular and biological compatibility with host alpha-synuclein influences fibril pathogenicity. Cell Rep 2016;16:3373–87

30. Waxman EA, Giasson BI. Specificity and regulation of casein kinase-mediated phosphorylation of alpha-synuclein. J Neuropathol Exp Neurol 2008;67:402–16

31. Waxman EA, Duda JE, Giasson BI. Characterization of antibodies that selectively detect alpha-synuclein in pathological inclusions. Acta Neuropathol 2008;116:37–46

32. Delic V, Chandra S, Abdelmotilib H, et al. Sensitivity and specificity of phospho-Ser129 alpha-synuclein monoclonal antibodies. J Comp Neurol 2018;526:1978–90

33. Matsutani S, Yamamoto N. Centrifugal innervation of the mammalian olfactory bulb. Anat Sci Int 2008;83:218–27

34. Rey NL, George S, Steiner JA, et al. Spread of aggregates after olfactory bulb injection of alpha-synuclein fibrils is associated with early neuronal loss and is reduced long term. Acta Neuropathol 2018;135:65–83

35. Jouandet ML, Hartenstein V. Basal telencephalic origins of the anterior commissure of the rat. Exp Brain Res 1983;50:183–92

36. Papp MI, Kahn JE, Lantos PL. Glial cytoplasmic inclusions in the CNS of patients with multiple system atrophy (striatonigral degeneration, olivopontocerebellar atrophy and Shy-Drager syndrome). J Neurol Sci 1989;94:79–100

37. Kuusisto E, Kauppinen T, Alafuzoff I. Use of p62/SQSTM1 antibodies for neuropathological diagnosis. Neuropathol Appl Neurobiol 2008;34: 169–80

38. Kovacs GG, Laszlo L, Kovacs J, et al. Natively unfolded tubulin polymerization promoting protein TPPP/p25 is a common marker of alpha-synucleinopathies. Neurobiol Dis 2004;17:155–62

39. Rey NL, Steiner JA, Maroof N, et al. Widespread transneuronal propagation of alpha-synucleinopathy triggered in olfactory bulb mimics prodromal Parkinson's disease. J Exp Med 2016;213:1759–78

40. Woerman AL, Oehler A, Kazmi SA, et al. Multiple system atrophy prions retain strain specificity after serial propagation in two different Tg(SNCA*A53T) mouse lines. Acta Neuropathol 2019;137:437–54

41. Peelaerts W, Bousset L, Baekelandt V, et al. a-Synuclein strains and seeding in Parkinson's disease, incidental Lewy body disease, dementia with Lewy bodies and multiple system atrophy: Similarities and differences. Cell Tissue Res 2018;373:195–212

42. Peelaerts W, Bousset L, Van der Perren A, et al. alpha-Synuclein strains cause distinct synucleinopathies after local and systemic administration. Nature 2015;522:340–4

43. Guo JL, Narasimhan S, Changolkar L, et al. Unique pathological tau conformers from Alzheimer's brains transmit tau pathology in nontransgenic mice. J Exp Med 2016;213:2635–54

44. Narasimhan S, Guo JL, Changolkar L, et al. Pathological tau strains from human brains recapitulate the diversity of tauopathies in nontransgenic mouse brain. J Neurosci 2017;37:11406–23

45. Arai T, Ueda K, Ikeda K, et al. Argyrophilic glial inclusions in the midbrain of patients with Parkinson's disease and diffuse Lewy body disease are immunopositive for NACP/alpha-synuclein. Neurosci Lett 1999;259:83–6

46. Wakabayashi K, Hayashi S, Yoshimoto M, et al. NACP/alpha-synuclein-positive filamentous inclusions in astrocytes and oligodendrocytes of Parkinson's disease brains. Acta Neuropathol 2000;99:14–20

47. Terada S, Ishizu H, Yokota O, et al. Glial involvement in diffuse Lewy body disease. Acta Neuropathol 2003;105:163–9

48. Braak H, Sastre M, Del Tredici K. Development of alpha-synuclein immunoreactive astrocytes in the forebrain parallels stages of intraneuronal pathology in sporadic Parkinson's disease. Acta Neuropathol 2007;114: 231–41

49. Hishikawa N, Hashizume Y, Yoshida M, et al. Widespread occurrence of argyrophilic glial inclusions in Parkinson's disease. Neuropathol Appl Neurobiol 2001;27:362–72

50. Terada S, Ishizu H, Haraguchi T, et al. Tau-negative astrocytic star-like inclusions and coiled bodies in dementia with Lewy bodies. Acta Neuropathol 2000;100:464–8

51. Osterberg VR, Spinelli KJ, Weston LJ, et al. Progressive aggregation of alpha-synuclein and selective degeneration of Lewy inclusion-bearing neurons in a mouse model of parkinsonism. Cell Rep 2015;10:1252–60

52. Djelloul M, Holmqvist S, Boza-Serrano A, et al. Alpha-synuclein expression in the oligodendrocyte lineage: An in vitro and in vivo study using rodent and human models. Stem Cell Rep 2015;5:174–84

53. Kaji S, Maki T, Kinoshita H, et al. Pathological endogenous alpha-synuclein accumulation in oligodendrocyte precursor cells potentially induces inclusions in multiple system atrophy. Stem Cell Rep 2018;10: 356–65

54. Mavroeidi P, Arvanitaki F, Karakitsou AK, et al. Endogenous oligodendroglial alpha-synuclein and TPPP/p25alpha orchestrate alpha-synuclein pathology in experimental multiple system atrophy models. Acta Neuropathol 2019;138:415–41

55. Tan FC, Hutchison ER, Eitan E, et al. Are there roles for brain cell senescence in aging and neurodegenerative disorders? Biogerontology 2014; 15:643–60

56. Karpowicz RJ Jr, Haney CM, Mihaila TS, et al. Selective imaging of internalized proteopathic alpha-synuclein seeds in primary neurons reveals mechanistic insight into transmission of synucleinopathies. J Biol Chem 2017;292:13482–97

57. Wenning GK, Stefanova N, Jellinger KA, et al. Multiple system atrophy: A primary oligodendrogliopathy. Ann Neurol 2008;64:239–46

58. Stefanova N, Wenning GK. Review: Multiple system atrophy: Emerging targets for interventional therapies. Neuropathol Appl Neurobiol 2016; 42:20–32

59. Song YJ, Lundvig DM, Huang Y, et al. p25alpha relocalizes in oligodendroglia from myelin to cytoplasmic inclusions in multiple system atrophy. Am J Pathol 2007;171:1291–303

60. Ubhi K, Low P, Masliah E. Multiple system atrophy: A clinical and neuropathological perspective. Trends Neurosci 2011;34:581–90

61. Cykowski MD, Coon EA, Powell SZ, et al. Expanding the spectrum of neuronal pathology in multiple system atrophy. Brain 2015;138: 2293–309

62. Reyes JF, Rey NL, Bousset L, et al. Alpha-synuclein transfers from neurons to oligodendrocytes. Glia 2014;62:387–98